LANGMUIR

pubs.acs.org/Langmuir Article

Colloidal Systems in Concentrated Electrolyte Solutions Exhibit Re-entrant Long-Range Electrostatic Interactions due to Underscreening

Haiyang Yuan, Wenjie Deng, Xiaolong Zhu, Guangming Liu,* and Vincent Stuart James Craig*

Cite This: *Langmuir* 2022, 38, 6164–6173 Read Online

ACCESS | Metrics & More | Article Recommendations | Supporting Information

ABSTRACT: Surface force measurements have revealed that at very high electrolyte concentrations as well as in neat and diluted ionic liquids and deep eutectic solvents, the range of electrostatic interactions is far greater than the Debye length. Here, we explore the consequences of this underscreening for soft-matter and colloidal systems by investigating the stability of nanoparticle dispersions, the self-assembly of ionic surfactants, and the thickness of soap films. In each case, we find clear evidence of re-entrant properties due to underscreening at high salt concentrations. Our results show that underscreening in concentrated electrolytes is a general phenomenon and is not dependent on confinement by macroscopic surfaces. The stability of systems at very high salinity due to underscreening may be beneficially applied to processes that currently use low-salinity water.

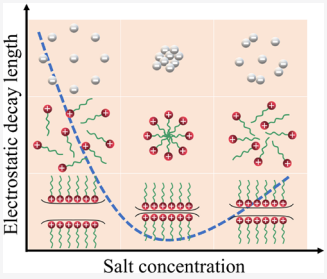

1. INTRODUCTION

Charge interactions play a central role in important technologies and biology. An important example is the stability of colloidal and nanoparticle solutions against flocculation as described by the renowned DLVO theory of Derjaguin and Landau[1] and Verwey and Overbeek.[2] Within this paradigm, the stability of colloidal systems is described as a balance between electrostatic repulsion between surfaces of like charges and the van der Waals attraction between the surfaces. At higher salt concentrations, the range of the electrostatic repulsion is screened more effectively, allowing the attractive van der Waals interactions to overcome the repulsive electrostatic forces, leading to flocculation. The self-assembly of ionic surfactants is also sensitive to the strength and range of electrostatic interactions. Self-assembly is promoted by hydrophobic interactions between the hydrocarbon (or fluorocarbon) tails of the surfactants and opposed by the Coulombic repulsion between the charged surfactant head-groups. This repulsion is screened upon increasing the salt concentration, leading to the onset of self-assembly at lower surfactant concentrations as measured by the critical micelle concentration (CMC).[3] Other examples of soft-matter systems that are sensitive to the range and strength of electrostatic interactions include the performance of batteries,[4] the viscoelasticity[5] and conformation of polyelectrolytes in solution,[6] the formation of polyelectrolyte multilayers,[7] the stability of emulsions,[8] the folding of proteins,[9] the crystallization of DNA,[10] and the drainage of foams.[11] Indeed, the majority of colloidal systems contain surfaces, polymers, or amphiphiles that are charged and are therefore strongly influenced by electrostatic interactions even in the presence of other interactions. Consequently, understanding these processes is dependent on theories and models of electrolytes in solution, which, being so important and challenging, is an important and substantial field of research.[12]

In the presence of other ions, the Coulomb interactions between ions are screened such that the interaction energy between charges is exponentially dependent on the separation. This is often expressed in terms of the Debye–Hückel[13] parameter κ_{DH}^2.

$$\kappa_{DH}^2 = \frac{q^2}{\varepsilon\varepsilon_0 k_B T} \sum_j n_j Z_j^2 \tag{1}$$

Here, the subscript "DH" is used to indicate that this parameter derives from the Debye–Hückel theory,[13] and n is the number density of the ion species j, with valence Z in solution. At low to moderate electrolyte concentrations, the exponential decay length is well described by the Debye length[13] λ_{DH}.

$$\lambda_{DH} = \kappa_{DH}^{-1} = \left(\frac{\varepsilon_0 \varepsilon k_B T}{q^2 \sum_j n_j Z_j^2} \right)^{1/2} \tag{2}$$

The Debye length is a measure of the range of electrostatic interactions. The Debye length decreases with an increase in salt concentration and is assumed to be independent of the

Received: March 2, 2022
Revised: April 26, 2022
Published: May 5, 2022

https://doi.org/10.1021/acs.langmuir.2c00519
Langmuir 2022, 38, 6164–6173

type of ion other than through the valency. It has been argued that the linear approximation used in the Debye−Hückel theory limits its applicability to low electrolyte concentrations in the millimolar range.[14,15] However, numerous surface force measurements at concentrations up to 0.1 M find that the decay in the interparticle force or the interaction energy between surfaces is in agreement with the Debye length.[16−20] Also, it is well argued on theoretical grounds, that linearization of the nonlinear Poisson−Boltzmann equation introduces only minor errors, and hence, the Debye−Hückel theory is applicable up to concentrations of ∼1 M for 1:1 electrolytes.[12] Ultimately, however, the applicability of the theory must break down at high concentrations as the granularity of the solvent and the finite size of the ions becomes important when the distance between ions is small. Experimentally, the decay length of electrostatic interactions at high electrolyte concentrations has rarely been explored as the expected very-short-range electrostatic interactions are extremely difficult to isolate and measure. Notably, the surprising observation of long-range electrostatic forces between surfaces immersed in ionic liquids[21,22] has recently led to a reassessment of this assumption. It was observed that for electrolytes consisting of monovalent ions at high salt concentrations, the electrostatic decay length is not clearly described by the Debye length and that the electrostatic decay length shows a minimum beyond which the range of electrostatic interactions increases with increasing electrolyte concentration. We call the concentration at which underscreening commences the minimum in the electrostatic decay length (MEDL). At higher concentrations, underscreening is apparent, and the range of the electrostatic interactions increases with concentration. Further, surface force apparatus measurements of the electrostatic decay length in aqueous electrolyte solutions exhibit underscreening,[21−25] as have force measurements performed using blinking optical tweezers[26] in non-aqueous solvent. Additionally, fluorescence studies that reveal the local concentration of ions between surfaces are consistent with underscreening in concentrated electrolyte solutions.[27] These surprising and fascinating observations have motivated the investigations reported here. The measured underscreening for 1:1 electrolytes was captured by Lee et al. in the following phenomenological expression[24]

$$\frac{\lambda_{HS}}{\lambda_{DH}} \approx \left(\frac{d'}{\lambda_{DH}}\right)^3 \tag{3}$$

where λ_{HS} is the electrostatic decay length above the MEDL and d' is the mean bare (unsolvated) ion diameter. Significantly, the presence of d' in eq 3 introduces an explicit ion specificity in the electrostatic decay length, $\lambda_{HS,}$ that is absent in the Debye length λ_{DH}. That is, at high concentrations, the electrostatic decay length becomes strongly dependent on the type of ion through the ion size in addition to the valency. The importance of the volume of the ions is made evident by rearrangement of eq 3; λ_{HS} is approximately given by

$$\lambda_{HS} \approx \frac{d'^3}{\lambda_{DH}^2} \approx \kappa_{DH}^2 d'^3 \tag{4}$$

We note that the expressions in eqs 3 and 4 are only applicable at high salt concentrations (above the MEDL). For simple 1:1 salts, observations reveal that the MEDL is ∼0.5 M where the λ_{DH} is ∼< 0.43 nm. Notably, for much larger ions, the discrepancy between the Debye length and the measured electrostatic decay length occurs at much lower concentrations (above 0.5 mM).[26] This leads to the hypothesis that for many soft-matter and colloidal systems, re-entrant behavior will be observed at high concentrations of simple electrolytes as underscreening leads to electrostatic interactions similar to those at much lower electrolyte concentrations. Further, multivalent ions have been shown to lead to underscreening at substantially lower concentrations.[28] A quantitative theoretical understanding of underscreening is not yet available. It is widely held that underscreening is at least in part due to ion−ion correlations arising from the finite size of ions,[29−35] but simulations have yet to produce the very large electrostatic decay lengths measured experimentally. Here, we investigate the stability of silica nanoparticles, the self-assembly of surfactants, and the thickness of soap films at high electrolyte concentrations to evaluate the electrostatic interactions evident in these systems in order to assess if underscreening is evident in colloidal systems.

2. EXPERIMENTAL SECTION

The salts were used as received without further purification.

2.1. Colloidal Stability Studies. Aqueous dispersions of silica nanoparticles were prepared by dilution to selected particle concentrations in the presence of a range of different electrolytes. Either negatively charged (40 wt %, Ludox HS-40) or positively charged (30 wt %, Ludox CL) SiO_2 nanoparticles with a diameter of ∼12 nm supplied by Sigma-Aldrich were used. The sign of the surface charge on these particles has been confirmed by measurements of electrophoretic mobility.[36] The negatively charged Ludox HS-40 particles are supplied at a concentration of 40 wt % and have ionizable surface silanol groups with sodium counterions. Impurities present include 0.01 wt % NaCl and 0.03 wt % Na_2SO_4. The positive charge on the Ludox CL SiO_2 nanoparticles (supplied at a concentration of 30 wt %) arises from an alumina coating and has chloride counterions. The particles were diluted substantially before use as indicated below. The transmittance of the samples was monitored using a UNICO 2802 UV/visible spectrophotometer with the wavelength set to 546 nm. The transmittance was used to follow the aggregation of the particles. When the particles were dispersed, the transmittance was high. Aggregation of the particles resulted in an increase in turbidity of the sample and a decrease in transmittance. This allowed the aggregation state of the particles to be probed. All the nanoparticle samples were stored in an incubator at ∼25 °C for ∼24 h before use. Prior to mounting the cell into the cell holder of the spectrophotometer, the sample was shaken by hand. The sample was equilibrated in a cell holder at ∼25 ± 0.1 °C for ∼20 min and then shaken again by hand immediately before each measurement.

2.2. Self-Assembly Studies. The aqueous solution and thin film properties of the surfactant tetradecyltrimethylammonium bromide (abbreviated here as MTAB and also known as C_{14}TAB) were studied in the presence of electrolytes. The surfactant was purchased from Aldrich and used without further purification. The surface tensions of surfactant solutions were measured by the pendant drop method using a CAM200 KSV contact angle goniometer at a temperature of 25 ± 1.0 °C. Measurements were repeated five times, and the average value reported. The estimated error in the reported values is ±0.1 mNm^{-1}. Solution densities, which are required in the calculation of the surface tension from the drop profile, were measured using an Anton Paar DMA35 densitometer.

2.3. Thin Film Studies. The process of thinning of surfactant films was studied using a Sheludko (also spelled Scheludko) thin film cell[37,38] with MTAB as the surfactant. The film was formed by injecting the surfactant solution into the film holder through a capillary. A Nikon AZ100M inverted microscope with a 5× objective lens was used to observe the thinning of films and captured using a Nikon Digital Sight DS9Fi1 color camera. The pixel size of the

https://doi.org/10.1021/acs.langmuir.2c00519
Langmuir 2022, 38, 6164−6173

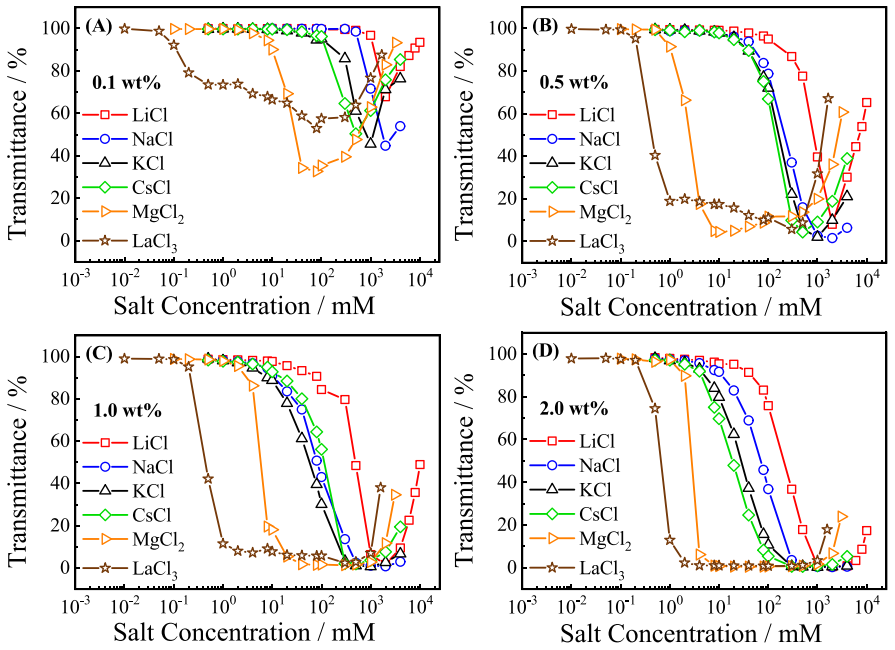

Figure 1. Transmittance of solutions containing negatively charged silica nanoparticles as a function of electrolyte concentration and type at different particle loadings of 0.1 wt % (A), 0.5 wt % (B), 1.0 wt % (C), and 2.0 wt % (D). Due to the small size of the primary particles (12 nm) compared to the wavelength of light (546 nm), the stable dispersions scatter a minimal amount of light. Addition of electrolyte results in flocculation and reduced transmittance. At very high salt concentrations, the transmittance increases. This is attributed to re-entrant colloidal stability driven by underscreening above the MEDL. The same transmittance data is plotted versus $[Cl^-]$ in Figure S2 of the Supporting Information.

captured images was 0.221 μm. A high-pressure mercury lamp was used for illumination. Monochromatic intensities were obtained from the color images using ImageJ software (National Institute of Health, USA). The film thickness, h, was determined in the usual manner[39−41] by analyzing the monochromatic intensity of reflected light from the liquid film (see the Supporting Information). The refractive index of the solution was obtained by adjusting the refractive index of the electrolyte solution to account for the surfactant using a dn/dC value of 0.15 cm^3/g.[42] The refractive indices of the electrolyte solutions were obtained by fitting a polynomial to the published data.[43] Tabulated values for the refractive index of aqueous $MgBr_2$ solutions could not be found, so values for $MgCl_2$ were used. We expect that this leads to a negligible overestimate of the film thickness.

The cell and syringe were soaked in distilled AR grade ethanol and then thoroughly rinsed with pure water before each solution was introduced. Sample solution was added to a reservoir under the film holder, and the whole cell was sealed to avoid accelerated film thinning due to evaporation from the film. When a new film was formed, the syringe was disconnected from the capillary to ensure that the liquid level in the capillary was equal to that of the film. Experiments were performed at 25 ± 1.0 ° C.

3. RESULTS AND DISCUSSION

3.1. Nanoparticle Stability. Colloidal silica particles in water are stabilized against flocculation by electrostatic repulsive forces arising from their similar surface charges. Thus, a sufficient reduction in the range or strength of the electrostatic interactions will allow the attractive van der Waals forces to cause the particles to flocculate. Important to our investigation here is the presence of short-range repulsive hydration forces, which prevent the particles from coming into a strongly attractive primary minimum, this enables the particles to be redispersed when the electrostatic repulsion is re-established.[19] The process of flocculation can be followed by observing a reduction in the transmission of light through a sample as the resultant increase in particle size enhances the amount of scattered light due to the strong dependence of light scattering intensity on particle radius. For spherical particles, Rayleigh scattering is applicable when the particle size is very much smaller than the wavelength of light and the relationship between the particle radius, r, and the intensity of the scattered light is $I \propto r^6$. Hence, the relationship between the particle volume V and the intensity of the scattered light is $I \propto V^2$. Thus for a floc formed from n monodisperse particles, the relationship between the number of particles and the change in scattering intensity is $\Delta I \propto n^2/n$. Hence, under Rayleigh conditions, flocs of particle size n scatter with n times more intensity than the dispersed particles from which they are formed. In our experiments, however, the conditions under which Rayleigh scattering is applicable are not always met; the same considerations apply, and flocculation leads to a large increase in the intensity of the scattered light.

In Figure 1, the influence of a range of electrolytes on the transmittance of dispersions of negatively charged silica particles is presented as a function of electrolyte concentration for a range of silica particle concentrations. Here, the co-ion is in every case the chloride ion, while the cation, which is the counterion, is varied. What is observed for each electrolyte is that as the concentration of electrolyte is increased, the transmittance is reduced, indicating that flocculation is occurring. With increasing electrolyte concentration, the transmittance reaches a minimum and then begins to increase, indicating that the silica nanoparticles are dispersed at very high electrolyte concentration. We attribute this trend to the influence of electrolyte on the range of the electrostatic interactions. Initially, there is a decrease in the electrostatic decay length with increasing electrolyte concentration that is consistent with the Debye length. However, at high electrolyte concentrations, the electrostatic decay length reaches a minimum at the MEDL and then increases with concentration.

https://doi.org/10.1021/acs.langmuir.2c00519
Langmuir 2022, 38, 6164−6173

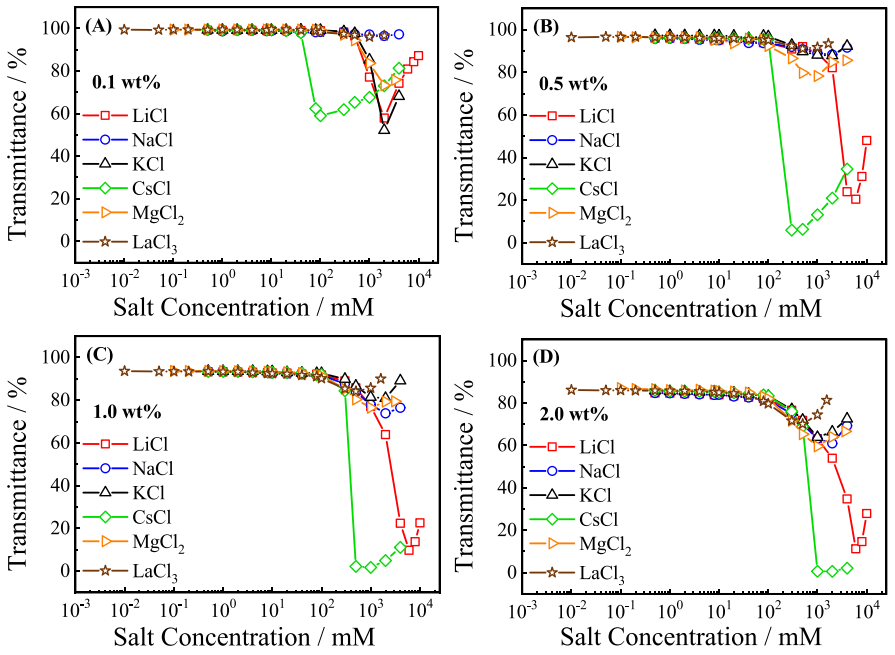

Figure 2. The transmittance of solutions containing positively charged alumina-coated silica nanoparticles as a function of electrolyte concentration and type at different particle loadings of 0.1 wt % (A), 0.5 wt % (B), 1.0 wt % (C), and 2.0 wt % (D). The stable dispersions scatter a minimal amount of light. The addition of electrolyte results in flocculation and reduced transmittance. At very high concentrations, the transmittance increases due to re-entrant colloidal stability. This is attributed to an increase in the electrostatic decay length above the MEDL.

This is consistent with recent studies showing underscreening at very high electrolyte concentrations.[21−25] The effect of the valency of the counterion has a strong influence on both the onset of flocculation and the re-entrant deflocculation. Additionally, the monovalent ions exhibit strong specific ion effects, with the effectiveness of flocculation being $Cs^+ > K^+ > Na^+ > Li^+$. This is consistent with the relative ion size and the lyotropic series[44] and the fundamental series of ion specificity[45,46] (but not with the accepted Hofmeister series,[45,47] noting that Hofmeister himself focused on the Na^+ and K^+ cations with the occasional use of Li^+ and did not report on Cs^+).[48] These specific ion effects are attributed to the influence of adsorption of the ions to the surface and the resulting reduction in the magnitude of the surface charge, with the larger ions adsorbing more effectively. This is supported by a decrease in the magnitude of the electrophoretic mobility with increasing electrolyte concentration (see Figure S1 in the Supporting Information). The greater effectiveness of the multivalent ions in flocculating the silica nanoparticles is attributed to both ion binding and electrostatic screening. The same trend, $Cs^+ > K^+ > Na^+ > Li^+$, is observed for the effectiveness of cations in redispersion and restabilization. This trend is consistent with the importance of ion size on the electrostatic decay length captured in eqs 3 and 4.

With increasing particle concentration, the onset of flocculation is observed at lower electrolyte concentration, consistent with expectations.[49] For particles of low Hamaker constants, the impact of neighboring particles on the interaction between a pair of particles is to reduce the total interaction energy and promote flocculation.[50] Re-entrant stabilization requires higher electrolyte concentrations at higher particle concentrations, consistent with restabilization by electrostatic forces.

The effect of the same series of electrolytes on the stability of positively charged alumina-coated silica nanoparticles is presented in Figure 2. With increasing electrolyte concentration, flocculation and re-entrant stability are evident for all electrolytes. Here, the counterion is in every case Cl^-. The screening of the positive surface potential will be insensitive to the valency of the cation (as they are largely excluded from the electrical double layer), and this is reflected in the data. With the exception of CsCl and LiCl, the effect of electrolyte on the particle stability is very similar when expressed as chloride concentration $[Cl^-]$ (see Figure S3 of the Supporting Information). While CsCl and LiCl are notably different to the other electrolytes, in all cases, re-entrant stability is observed at high salt concentrations. This is consistent with the hypothesis that the re-entrant colloidal stability is driven by underscreening above the MEDL.

In comparing the negatively charged nanoparticles with the positively charged nanoparticles, it is evident that the flocculation of the negatively charged nanoparticles occurs at lower concentrations and to a far greater extent. This is consistent with the adsorption of the cations to the negatively charged nanoparticles and a corresponding lowering of the surface potential. In the case of positively charged nanoparticles, the flocculation onset is strongly ion-specific. In comparison, the concentration at which re-entrant stability is observed is similar for all electrolytes for the positively charged nanoparticles. The trend observed in the re-entrant solubilization is similar to that expected based on the influence of ion size captured in eqs 3 and 4, suggesting that the redispersion is not strongly influenced by the specifics of the surface interactions but rather is a property of the bulk electrolyte and is a result of an increase in electrostatic decay length. At increasing particle concentrations, flocculation was observed at lower electrolyte concentrations as was seen for the negatively charged silica particles. This is in contrast to the observation of positively charged nanoparticles in the presence of CsCl, which shows the opposite trend. This suggests that flocculation by

https://doi.org/10.1021/acs.langmuir.2c00519
Langmuir 2022, 38, 6164−6173

CsCl is mediated by direct adsorption and that the level of adsorption is sufficient to deplete the overall concentration of the electrolyte. As this is not observed for the other electrolytes, this implies that the Cs^+ ions are adsorbing (i.e., co-ion adsorption) in concert with Cl^- ions despite the cationic nature of the surface. This could be related to the large polarizability of Cs^+ ions.

3.2. Self-Assembly of Surfactants. The self-assembly of ionic surfactants is driven by hydrophobic interactions and countered by the repulsion between the charged head-groups, which are brought into close proximity upon micellization. Therefore, the self-assembly of ionic surfactants is sensitive to the addition of electrolyte, which mediates the range of electrostatic repulsions between surfactant head-groups. Additionally, electrolytes can influence self-assembly through Hofmeister effects[48] that influence the solubility of the surfactant through salting-out and salting-in processes. Here, the influence of the electrolytes KBr, NaBr, and $MgBr_2$ on the surface tension of aqueous myristyltrimethylammonium bromide (MTAB) solutions has been investigated to determine the influence of electrolyte on the critical micelle concentration (CMC) and the surface excess. When the surface tension is plotted against the log of the surfactant concentration, the surface tension initially decreases gradually and then linearly with the log of surfactant concentration. The CMC is traditionally determined from the break in this linear relationship when the surface tension reaches a limiting value as shown in the top panel in Figure 3. This sharp break, commonly observed at low electrolyte concentration, is due to the sudden onset of micellization and enables the CMC to be determined with little ambiguity. In the presence of concentrated electrolyte, the linear decrease in surface tension with the log of surfactant concentration is still seen, but it does not end in a sharp break at the limiting value of the surface tension. Rather, there is a broader transition that indicates that the onset of micellization is gradual, and hence, the determination of the CMC by surface tensiometry is inherently ambiguous. A reliable method is required to determine the CMC in a manner that enables comparison between solutions with different concentrations and types of electrolytes. We have chosen to define the CMC as the intersection of a line fitted to the linear portion with a horizontal line defined by the limiting surface tension as shown in the bottom panel of Figure 3. The advantage of this method is that it allows for a robust and consistent determination of the CMC across all concentrations of electrolyte. We acknowledge that in the absence of an understanding of the details of the micellization process, the CMC may be defined in other ways such as the concentration at which the data first breaks from the linear trend, but it is difficult to define this concentration, so we have chosen to use the more quantitatively robust method. We note here that it is widely recognized that different techniques (e.g., surface tension, conductivity, turbidity, fluorescence, dye solubilization, and osmotic pressure) give rise to differing values for the CMC, but the comparison of CMCs is admissible within a method.

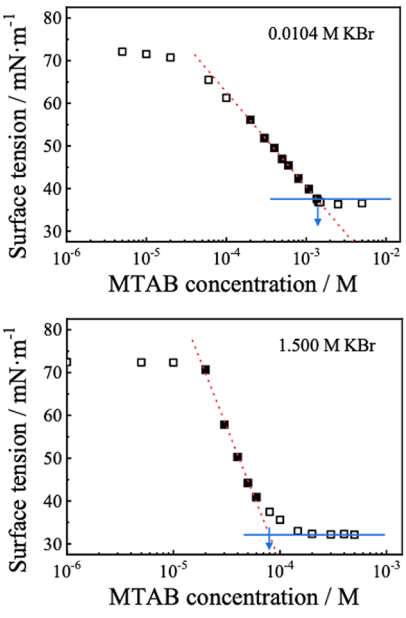

Figure 3. Illustration of the method used for the determination of the critical micelle concentration from the measured surface tension versus MTAB concentration (log scale) in the presence of 0.0104 M KBr (top) and 1.500 M KBr (bottom). In the presence of high concentrations of electrolyte, the surface tension data does not show a sharp break from the linear data as seen at low electrolyte concentrations. In both cases, the CMC, as indicated by the arrow, was determined from the intersection of a line fitted to the linear portion of the slope (filled symbols) and a horizontal line defined by the limiting surface tension.

The CMCs of MTAB solutions as a function of electrolyte concentration for KBr, NaBr, and $MgBr_2$ are presented in Figure 4. In each case, the addition of electrolyte led to the same trend in the CMC. Initially, added electrolyte reduced the CMC significantly (the CMC of MTAB in the absence of added electrolyte is ~3.65 mM). This well-known effect is attributed to both counterion binding and electrostatic screening between head-groups. At higher concentrations of between ~1.0 and 2.5 M, the CMC reached a minimum value, which is consistent with the electrostatic interactions between head-groups being highly screened. At very high concentrations of electrolyte, the CMC increased substantially. This is attributed to an increase in electrostatic interactions between head-groups, consistent with underscreening. The effect of electrolytes on surfactant surface tension has been previously investigated extensively, but we know of no prior studies that systematically investigate the surface tension of surfactant solutions in concentrated electrolytes.

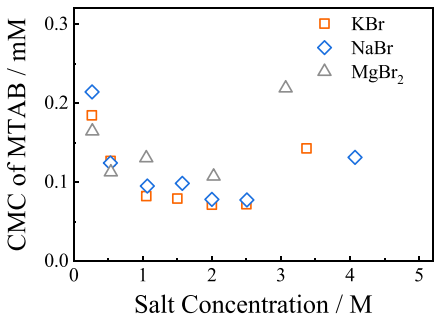

Figure 4. The critical micelle concentration (CMC) of MTAB in the presence of electrolyte. With increasing electrolyte concentration, the CMC shows a minimum before increasing at very high concentrations of electrolyte. This trend is consistent with an initial decrease in the electrostatic decay length and an increase in the electrostatic decay length at very high salt concentrations.

https://doi.org/10.1021/acs.langmuir.2c00519
Langmuir 2022, 38, 6164−6173

It is notable that the CMC values at very high electrolyte concentrations are comparable to those at electrolyte concentrations below 0.5 M. The influence of NaBr and KBr on the CMC is similar over most of the concentration range but differs considerably at very high concentrations, where the effectiveness of increasing the CMC is in the order $Mg^{2+} > K^+ > Na^+$. This is consistent with the expectation from eqs 3 and 4, as the larger cation (K^+) results in greater underscreening and the valency of the Mg^{2+} ion is expected to dominate the cation size effects. In addition to electrostatic interactions, the addition of electrolyte at these concentrations will also impact the solubility of the hydrocarbon chain of the surfactant. The bromide anion is known to increase the solubility or "salt-in" organic species. This salting-in effect, which increases with electrolyte concentration, will inhibit micellization and increase the CMC. This enhances the impact of underscreening (which also raises the CMC) and therefore moves the minimum in the CMC to higher concentrations. The cations also impact the solubility of organic species by decreasing the solubility (salting-out). The different behavior at high salt concentrations observed here is primarily attributed to the impact of ion types on underscreening rather than salting-in effects. It has been suggested that the underscreening observed in surface force measurements and in fluorescence studies may be associated with the confinement of liquids.[32,51,52] However, the influence of electrolyte on the CMC seen here demonstrates for the first time that underscreening is evident in a system not confined by surfaces.

The surface tension data was analyzed using the Gibbs adsorption isotherm to evaluate the surface excess, Γ_B (mol L^{-1} m^{-2}), at the air−solution interface and the area per surfactant molecule, a_0 (nm^2) (see the Supporting Information). At high concentrations, KBr exhibits an increase in area per molecule, consistent with an increase in the electrostatic decay length. This increase is not seen with either NaBr or $MgBr_2$. We posit that this is due to the relative salting-out effectiveness of the salts, which is $MgBr_2 > NaBr > KBr$.[53]

3.3. Soap Film Thickness. When a soap film is allowed to drain a film forms between the plateau borders, which is plane-parallel with a thickness determined by the disjoining pressure in the film (i.e., the repulsive surface forces) and the suction pressure in the plateau border. In the presence of ionic surfactants, the surfaces of the film acquire a net surface charge and the dominant contribution to the disjoining pressure at thicknesses greater than ~5 nm is electrostatic repulsion. Films of this thickness reflect only little light due to destructive interference between light reflected from the front and the back of the film. Consequently, they appear dark and are known as common black films. As the addition of electrolyte strongly influences the range of the electrostatic interactions, this manifests as changes in the film thickness of common black films, which can be followed through measurement of the reflectance of the film as shown in Figure 5.

The measured film thickness as a function of electrolyte concentration and type is shown in Figure 6 for MTAB at 0.5 of the CMC concentration. A clear trend of increasing film thickness is evident for electrolyte concentrations above 1 M. This is attributed to an increase in disjoining pressure resulting from underscreening. As the CMC is dependent on the electrolyte concentration and type (see Figure 4), the MTAB concentration is necessarily different for each data point (see Table S1 in the Supporting Information for the MTAB concentrations employed). The MTAB has only a minimal

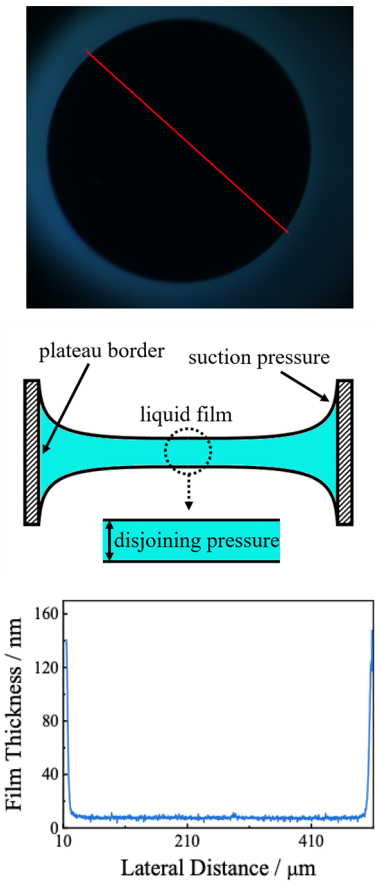

Figure 5. Optical micrograph of a soap film in the presence of 0.20 mM MTAB and 3.07 M $MgBr_2$ (top). A schematic of the soap film showing the plateau borders where the soap film meets the frit. The curvature in the plateau border region causes a suction pressure that acts to thin the film; this is balanced by the disjoining pressure in the film, which arises from the surface forces (middle). The reflectance data obtained from the micrograph is used to derive the film thickness. The film is plane-parallel in the black region as shown by the constant thickness (bottom).

effect on the ionic strength of the solution as the electrolyte concentration is much greater. If the MTAB concentration was held constant, the addition of electrolyte would induce micellization, and hence, micelles would be present in some cases but not others. As the presence of micelles has the potential to alter the range of the repulsive forces via electrostatic repulsion, this approach was not employed; rather, the surfactant concentration was maintained at half or twice the CMC to aid comparison across electrolyte concentrations.

The effect of electrolyte concentration and type on the thickness of MTAB films at 2.0 times the CMC is shown in Figure 7. As with the measurements below the CMC, an increasing film thickness with increasing electrolyte concentration is observed above 1 M. The data suggest that the electrostatic decay length minimum is around 1 M.

Measurements of film thickness are more likely than CMC measurements to reveal the concentration at which the electrostatic decay length begins to increase as salting-in effects are less likely to influence the measurements. However, the addition of salt influences the degree of ionization of surfactants.[54] At low salt concentrations, the degree of ionization is reduced with increasing salt concentration and

https://doi.org/10.1021/acs.langmuir.2c00519
Langmuir 2022, 38, 6164−6173

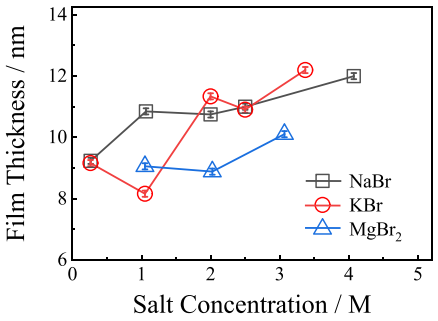

Figure 6. Measured film thickness at 0.5× CMC of MTAB in the presence of NaBr, KBr, and $MgBr_2$. The error in the measured thickness from uncertainty in the refractive index is estimated to be ±1.0 nm, while the standard error in these measurements is less than the size of the data points. These measurements are made on black films that have been allowed to thin to a steady thickness that is determined by the forces within the film. For all three salts, the thickness of the film is observed to increase with increasing electrolyte concentration, indicating an increase in the repulsive forces between the two solution−air interfaces. This is consistent with an increase in the range of electrostatic interactions with increasing electrolyte concentration above the MEDL. At millimolar ionic strengths, the thickness of the film closely follows the Debye length (see the Supporting Information).

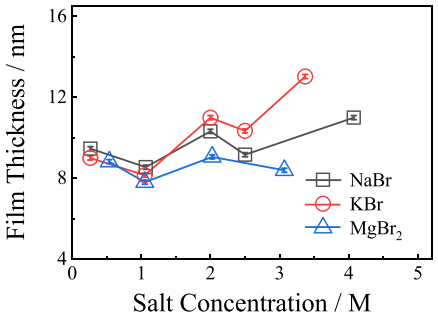

Figure 7. Measured film thickness at 2.0× CMC of MTAB in the presence of NaBr, KBr, and $MgBr_2$. The error in the measured thickness from uncertainty in the refractive index is estimated to be ±1.0 nm, while the standard error in these measurements is less than the size of the data points. These measurements are made on common black films that have been allowed to thin to a steady thickness that is determined by the forces within the film. The thickness of the film is observed to increase with increasing electrolyte concentration beyond 1 M, indicating an increase in the repulsive forces between the two solution−air interfaces. This is consistent with an increase in the range of electrostatic interactions with increasing electrolyte concentration above the MEDL. At millimolar ionic strengths, the thickness of the film closely follows the Debye length (see the Supporting Information).

is ion-specific, but little is known about the degree of ionization at very high salt concentrations. Determining the MEDL is important as it defines the concentration at which the Debye length regime is superseded by underscreening, but the experiments reported here are influenced by other factors, so they are only able to give an estimate of this minimum. At surfactant concentrations above the CMC, the presence of micelles in the thin film can give rise to short-range structural forces. Additionally, changes in electrolyte concentration give rise to changing electrostatic interactions between charged surfactant head-groups, and this can drive changes in the shape of the micelle. When the electrostatic interactions are long-ranged, micelles tend to be more spherical. We currently do not have direct measurements of how the addition of high concentrations of electrolyte influence the shape of MTAB micelles or ionic micelles in general. We would like to investigate this in the future. As the micelles generally have dimensions of <3 nm, we do not believe that short-range structural forces arising from micelles are evident in our measurements reported here. Further, no evidence was seen of step changes in the thin film thickness that would be expected when layers of micelles are displaced upon thinning of the film, and we observe the same trends above and below the CMC.

The knowledge that electrostatic interactions are underscreened in concentrated aqueous electrolytes,[23−25] ionic liquids,[21,22] and deep eutectic solvents[55] demands that previous investigations in such systems be reevaluated and suggests a number of new opportunities and applications. One particular area in which new possibilities arise is in the stability of colloidal systems in concentrated electrolytes. Here, we have shown that the stability of nanoparticles, the self-assembly of surfactants, and the thickness of soap films demonstrate re-entrant stability conferred by an increase in the range of electrostatic interactions at high salt concentrations, this complements previous work demonstrating that polyelectrolytes exhibit re-entrant stability,[6] and the demonstration that charged micelles in deep eutectic solvents exhibit long-range electrostatic interactions, far greater than expected from the Debye length.[55] The implication is that electrostatically stabilized colloidal systems occur both at low and very high salt concentrations, and as such, electrostatically stabilized colloidal systems can be realized in hypersaline waste streams. It is notable that the onset of underscreening occurs for simple salts when the Debye length is approximately the size of the ions,[21,23−25] which supports suggestions that the effect may be due to ion−ion correlations.[56,57] However, for much larger ions (~10 times larger), the onset occurs when the Debye length is two orders of magnitude larger than the ion size,[26] and in this case, the dependence of the electrostatic decay length is not described by eqs 3 and 4. Here, the mechanism by which the range of the interaction is extended may be different. The authors attribute it to charge regulation, which leads to a decrease in surface charge as the surfaces approach. Further, they show that the effective surface charge begins to decrease at the onset of underscreening. However, if this was the dominant mechanism operating, the interaction would not decay exponentially and the interaction measured at a concentration of 600 μM would not intersect with that measured at 450 μM at larger separations, as seen in Figure 1 of their paper.[26] Thus, we suggest that this is a related phenomenon, but underscreening is not the sole cause of the extended decay length measured and reported in their work. What is not clear at this stage is if the extended decay lengths they measured using weak electrolytes in which only 1 in ~30,000 molecules are ionized have the same origin as those reported for the simple electrolytes. The development of new methods that directly measure the electrostatic decay length or the ion profiles near surfaces[27] are important. The quantification of decay lengths for a wide range of salts across a range of concentrations is required to rigorously determine the importance of valency and ion type on the onset of underscreening. This knowledge will contribute to the development of a theoretical understanding of the origins of underscreening. Such knowledge is highly relevant to advanced battery technology, particularly with regard to developments in which very high salt concentrations are being employed.[4,58,59]

https://doi.org/10.1021/acs.langmuir.2c00519
Langmuir 2022, 38, 6164−6173

It is also important in understanding the ecology and formation of sediments in hypersaline lakes[60] and the dewatering of sludge in hypersaline waste streams.[61] Moreover, these effects may be evident in lyotropic liquid crystals formed from ionic surfactants due to the high concentration of ions in these systems. Here, long-range electrostatic interactions combined with anisotropic electrostatic screening and elastic interactions could be used to tune effective pair potentials between colloidal particles.[62]

4. CONCLUSIONS

Electrostatic interactions play a fundamentally important role in the structure, properties, and function of soft-matter systems, and consequently, these systems are sensitive to the concentration of electrolytes, which screens these interactions. At concentrations up to ∼0.5 M for simple 1:1 salts, the exponential decay length of electrostatic interactions is well described by the Debye length. At higher concentrations, the range of the electrostatic interactions increase with increasing electrolyte concentration, reversing the trend observed at low electrolyte concentrations. As such, the structure and properties of soft-matter systems should exhibit re-entrant behavior in which the properties evident at low electrolyte concentrations are re-established at very high electrolyte concentrations. In this work, the stability of nanoparticle suspensions, the critical micelle concentration, and the thickness of thin soap films have all been shown to demonstrate this re-entrant behavior, revealing that colloidal systems can be electrostatically stabilized at high salt concentrations. This is commensurate with earlier work on the re-entrant stability of polyelectrolytes and provides further evidence that underscreening is not induced by confinement. While it is expected that the applicability of the Debye−Hückel theory of electrolytes should break down at sufficiently high electrolyte concentrations, it is not yet clear why the degree of underscreening is so great at high electrolyte concentrations. Regardless, the strength of underscreening observed opens up a wide range of possibilities and potential new applications for soft-matter and colloidal systems in hypersaline solutions.

■ ASSOCIATED CONTENT

Supporting Information

The Supporting Information is available free of charge at https://pubs.acs.org/doi/10.1021/acs.langmuir.2c00519.

Electrophoretic mobility of negatively charged silica nanoparticles; transmittance of silica suspensions in a range of electrolytes plotted as a function of chloride concentration; surface excess and area per surfactant molecule at the air−solution interface; salt and surfactant concentrations employed in the thin film studies; comparison of thin film thickness and Debye length in surfactant films at low concentrations (PDF)

■ AUTHOR INFORMATION

Corresponding Authors

Guangming Liu − *Department of Chemical Physics, Key Laboratory of Surface and Interface Chemistry and Energy Catalysis of Anhui Higher Education Institutes, University of Science and Technology of China, Hefei 230026, P. R. China;* orcid.org/0000-0003-2455-1395; Email: gml@ustc.edu.cn

Vincent Stuart James Craig − *Department of Chemical Physics, Key Laboratory of Surface and Interface Chemistry and Energy Catalysis of Anhui Higher Education Institutes, University of Science and Technology of China, Hefei 230026, P. R. China; Department of Applied Mathematics, Research School of Physics, The Australian National University, Canberra, ACT 2601, Australia;* orcid.org/0000-0002-8048-8397; Email: vince.craig@anu.edu.au

Authors

Haiyang Yuan − *Department of Chemical Physics, Key Laboratory of Surface and Interface Chemistry and Energy Catalysis of Anhui Higher Education Institutes, University of Science and Technology of China, Hefei 230026, P. R. China;* orcid.org/0000-0002-9554-8428

Wenjie Deng − *Department of Chemical Physics, Key Laboratory of Surface and Interface Chemistry and Energy Catalysis of Anhui Higher Education Institutes, University of Science and Technology of China, Hefei 230026, P. R. China*

Xiaolong Zhu − *State Key Laboratory of Fire Science, University of Science and Technology of China, Hefei 230026, P. R. China*

Complete contact information is available at: https://pubs.acs.org/10.1021/acs.langmuir.2c00519

Notes

The authors declare no competing financial interest.

■ ACKNOWLEDGMENTS

The financial support of the National Natural Science Foundation of China (21873091 and 52033001), the Youth Innovation Promotion Association of CAS (Y201769), the National Synchrotron Radiation Laboratory (UN2018LHJJ), and the Fundamental Research Funds for the Central Universities (WK2480000007) is acknowledged. Funding from the Australian Research Council through the Discovery Program (DP190100788) is greatly appreciated. The support of USTC, Hefei for V.S.J.C. through an international visiting professorship (2018B VR11) is gratefully acknowledged. V.S.J.C. acknowledges fruitful discussions with Rolland Kjellander.

■ REFERENCES

(1) Derjaguin, B. V.; Landau, L. Theory of the stability of strongly charged lyophobic sols and of the adhesion of strongly charged particles in solution of electrolytes. *Acta. Physicochem. URSS* **1941**, *14*, 633.

(2) Verwey, E. J. W.; Overbeek, J. T. G. *Theory of the Stability of Lyophobic Colloids*; Elsevier: Amsterdam, The Netherlands, 1948.

(3) Israelachvili, J. N.; Mitchell, D. J.; Ninham, B. W. Theory of self-assembly of hydrocarbon amphiphiles into micelles and bilayers. *J. Chem. Soc., Faraday Trans.* **1976**, *2*, 1525−1568.

(4) Borodin, O.; Self, J.; Persson, K. A.; Wang, C.; Xu, K. Uncharted Waters: Super-Concentrated Electrolytes. *Joule* **2020**, *4*, 69−100.

(5) Turkoz, E.; Perazzo, A.; Arnold, C. B.; Stone, H. A. Salt type and concentration affect the viscoelasticity of polyelectrolyte solutions. *Appl. Phys. Lett.* **2018**, *112*, 203701.

(6) Liu, G.; Parsons, D.; Craig, V. S. J. Re-entrant swelling and redissolution of polyelectrolytes arises from an increased electrostatic decay length at high salt concentrations. *J. Colloid Interface Sci.* **2020**, *579*, 369−378.

(7) Wong, J. E.; Zastrow, H.; Jaeger, W.; von Klitzing, R. Specific Ion versus Electrostatic Effects on the Construction of Polyelectrolyte Multilayers. *Langmuir* **2009**, *25*, 14061−14070.

(8) Kundu, P.; Agrawal, A.; Mateen, H.; Mishra, I. M. Stability of oil-in-water macro-emulsion with anionic surfactant: Effect of electrolytes and temperature. *Chem. Eng. Sci.* **2013**, *102*, 176−185.
(9) Lindman, S.; Xue, W.-F.; Szczepankiewicz, O.; Bauer, M. C.; Nilsson, H.; Linse, S. Salting the Charged Surface: pH and Salt Dependence of Protein G B1 Stability. *Biophys. J.* **2006**, *90*, 2911−2921.
(10) Seo, S. E.; Girard, M.; De La Cruz, M. O.; Mirkin, C. A. The Importance of Salt-Enhanced Electrostatic Repulsion in Colloidal Crystal Engineering with DNA. *ACS Cent. Sci.* **2019**, *5*, 186−191.
(11) Ruckenstein, E.; Bhakta, A. Effect of Surfactant and Salt Concentrations on the Drainage and Collapse of Foams Involving Ionic Surfactants. *Langmuir* **1996**, *12*, 4134−4144.
(12) Kontogeorgis, G. M.; Maribo-Mogensen, B.; Thomsen, K. The Debye-Hückel theory and its importance in modeling electrolyte solutions. *Fluid Phase Equilib.* **2018**, *462*, 130−152.
(13) Debye, P. The theory of electrolytes I. The lowering of the freezing point and related occurrences. *Phys. Z.* **1923**, *24*, 185−206.
(14) Alves, K. C. N.; Pessôa Filho, P. A. An assessment on the use of the Debye-Hückel equation for the thermodynamic modeling of aqueous systems containing polymers and salts. *Braz. J. Chem. Eng.* **2010**, *27*, 315−325.
(15) Olivares, W.; McQuarrie, D. A. On the theory of ionic solutions. *Biophys. J.* **1975**, *15*, 143−162.
(16) Ducker, W. A.; Senden, T. J.; Pashley, R. M. Direct Measurement of Colloidal Forces Using an Atomic Force Microscope. *Nature* **1991**, *353*, 239−241.
(17) Israelachvili, J. N.; Adams, G. E. Measurement of forces between 2 mica surfaces in aqueous-electrolyte solutions in range 0-100 nm. *J. Chem. Soc., Faraday Trans.* **1978**, *74*, 975−1001.
(18) Walsh, R. B.; Evans, D.; Craig, V. S. J. Surface Force Measurements between Titanium Dioxide Surfaces Prepared by Atomic Layer Deposition in Electrolyte Solutions Reveal Non-DLVO Interactions: Influence of Water and Argon Plasma Cleaning. *Langmuir* **2014**, *30*, 2093−2100.
(19) Eom, N.; Parsons, D. F.; Craig, V. S. J. Roughness in Surface Force Measurements: Extension of DLVO Theory To Describe the Forces between Hafnia Surfaces. *J. Phys. Chem. B* **2017**, *121*, 6442−6453.
(20) Sedev, R.; Exerowa, D. DLVO and non-DLVO surface forces in foam films from amphiphilic block copolymers. *Adv. Colloid Interface Sci.* **1999**, *83*, 111−136.
(21) Gebbie, M. A.; Smith, A. M.; Dobbs, H. A.; Lee, A. A.; Warr, G. G.; Banquy, X.; Valtiner, M.; Rutland, M. W.; Israelachvili, J. N.; Perkin, S.; Atkin, R. Long range electrostatic forces in ionic liquids. *Chem. Commun.* **2017**, *53*, 1214−1224.
(22) Gebbie, M. A.; Valtiner, M.; Banquy, X.; Fox, E. T.; Henderson, W. A.; Israelachvili, J. N. Ionic liquids behave as dilute electrolyte solutions. *Proc. Natl. Acad. Sci. U. S. A.* **2013**, *110*, 9674−9679.
(23) Smith, A. M.; Lee, A. A.; Perkin, S. The Electrostatic Screening Length in Concentrated Electrolytes Increases with Concentration. *J. Phys. Chem. Lett.* **2016**, *7*, 2157−2163.
(24) Lee, A. A.; Perez-Martinez, C. S.; Smith, A. M.; Perkin, S. Scaling Analysis of the Screening Length in Concentrated Electrolytes. *Phys. Rev. Lett.* **2017**, *119*, No. 026002.
(25) Lee, A. A.; Perez-Martinez, C. S.; Smith, A. M.; Perkin, S. Underscreening in concentrated electrolytes. *Faraday Discuss.* **2017**, *199*, 239−259.
(26) Waggett, F.; Shafiq, M.; Bartlett, P. Failure of Debye-Hückel Screening in Low-Charge Colloidal Suspensions. *Colloids Interfaces* **2018**, *2*, 51.
(27) Gaddam, P.; Ducker, W. Electrostatic Screening Length in Concentrated Salt Solutions. *Langmuir* **2019**, *35*, 5719−5727.
(28) Smith, A. M.; Maroni, P.; Trefalt, G.; Borkovec, M. Unexpectedly Large Decay Lengths of Double-Layer Forces in Solutions of Symmetric, Multivalent Electrolytes. *J. Phys. Chem. B* **2019**, *123*, 1733−1740.
(29) Kjellander, R. The intimate relationship between the dielectric response and the decay of intermolecular correlations and surface forces in electrolytes. *Soft Matter* **2019**, *15*, 5866−5895.
(30) Krucker-Velasquez, E.; Swan, J. W. Underscreening and hidden ion structures in large scale simulations of concentrated electrolytes. *J. Chem. Phys.* **2021**, *155*, 134903.
(31) Jones, P.; Coupette, F.; Härtel, A.; Lee, A. A. Bayesian unsupervised learning reveals hidden structure in concentrated electrolytes. *J. Chem. Phys.* **2021**, *154*, 134902.
(32) Coles, S. W.; Park, C.; Nikam, R.; Kanduč, M.; Dzubiella, J.; Rotenberg, B. Correlation Length in Concentrated Electrolytes: Insights from All-Atom Molecular Dynamics Simulations. *J. Phys. Chem. B* **2020**, *124*, 1778−1786.
(33) Adar, R. M.; Safran, S. A.; Diamant, H.; Andelman, D. Screening length for finite-size ions in concentrated electrolytes. *Phys. Rev. E* **2019**, *100*, No. 042615.
(34) Rotenberg, B.; Bernard, O.; Hansen, J.-P. Underscreening in ionic liquids: a first principles analysis. *J. Phys.: Condens. Matter* **2018**, *30*, No. 054005.
(35) Lee, S. S.; Koishi, A.; Bourg, I. C.; Fenter, P. Ion correlations drive charge overscreening and heterogeneous nucleation at solid−aqueous electrolyte interfaces. *Proc. Natl. Acad. Sci. U. S. A.* **2021**, *118*, No. e2105154118.
(36) Van Der Meeren, P.; Saveyn, H.; Bogale Kassa, S.; Doyen, W.; Leysen, R. Colloid-membrane interaction effects on flux decline during cross-flow ultrafiltration of colloidal silica on semi-ceramic membranes. *Phys. Chem. Chem. Phys.* **2004**, *6*, 1408.
(37) Henry, C. L.; Karakashev, S. I.; Nguyen, P. T.; Nguyen, A. V.; Craig, V. S. J. Ion Specific Electrolyte Effects on Thin Film Drainage in Nonaqueous Solvents Propylene Carbonate and Formamide. *Langmuir* **2009**, *25*, 9931−9937.
(38) Sheludko, A. Thin liquid films. *Adv. Colloid Interface Sci.* **1967**, *1*, 391−464.
(39) Kristen, N.; von Klitzing, R. Effect of polyelectrolyte/surfactant combinations on the stability of foam films. *Soft Matter* **2010**, *6*, 849−861.
(40) Exerowa, D.; Kolarov, T.; Khristov, K. Direct measurement of disjoining pressure in black foam films. I. Films from an ionic surfactant. *Colloids Surf.* **1987**, *22*, 161−169.
(41) Karakashev, S. I.; Nguyen, A. V.; Manev, E. D. A novel technique for improving interferometric determination of emulsion film thickness by digital filtration. *J. Colloid Interface Sci.* **2007**, *306*, 449−453.
(42) Pagac, E. S.; Prieve, D. C.; Tilton, R. D. Kinetics and mechanism of cationic surfactant adsorption and coadsorption with cationic polyelectrolytes at the silica− water interface. *Langmuir* **1998**, *14*, 2333−2342.
(43) CRC. *Handbook of Chemistry and Physics*; 80th ed.; CRC Press LLC, 2000.
(44) Voet, A. Quantitative lyotropy. *Chem. Rev.* **1937**, *20*, 169−179.
(45) Mazzini, V.; Craig, V. S. J. What is the fundamental ion-specific series for anions and cations? Ion specificity in standard partial molar volumes of electrolytes and electrostriction in water and non-aqueous solvents. *Chem. Sci.* **2017**, *8*, 7052−7065.
(46) Mazzini, V.; Craig, V. S. J. Corriegendum What is the fundamental ion-specific series for anions and cations? Ion specificity in standard partial molar volumes of electrolytes and electrostriction in water and non-aqueous solvents (vol 8, pg 7052, 2017). *Chem. Sci.* **2019**, *10*, 3430−3433.
(47) Mazzini, V.; Craig, V. S. J. Specific-ion effects in non-aqueous systems. *Curr. Opin. Colloid Interface Sci.* **2016**, *23*, 82−93.
(48) Kunz, W.; Henle, J.; Ninham, B. W. Zur Lehre von der Wirkung der Salze' (about the science of the effect of salts): Franz Hofmeister's historical papers. *Curr. Opin. Colloid Interface Sci.* **2004**, *9*, 19−37.
(49) Kaldasch, J.; Laven, J.; Stein, H. N. Equilibrium Phase Diagram of Suspensions of Electrically Stabilized Colloidal Particles. *Langmuir* **1996**, *12*, 6197−6201.

https://doi.org/10.1021/acs.langmuir.2c00519
Langmuir 2022, 38, 6164−6173

(50) Hsu, J.-P.; Liu, B.-T. Critical Coagulation Concentration of a Colloidal Suspension at High Particle Concentrations. *J. Phys. Chem. B* **1998**, *102*, 334−337.
(51) Zeman, J.; Kondrat, S.; Holm, C. Bulk ionic screening lengths from extremely large-scale molecular dynamics simulations. *Chem. Commun.* **2020**, *56*, 15635−15638.
(52) Zeman, J.; Kondrat, S.; Holm, C. Ionic screening in bulk and under confinement. *J. Chem. Phys.* **2021**, *155*, 204501.
(53) Xie, W.-H.; Shiu, W.-Y.; Mackay, D. A review of the effect of salts on the solubility of organic compounds in seawater. *Mar. Environ. Res.* **1997**, *44*, 429−444.
(54) Kumar, B.; Tikariha, D.; Ghosh, K. K. Effects of Electrolytes on Micellar and Surface Properties of Some Monomeric Surfactants. *J. Dispersion Sci. Technol.* **2012**, *33*, 265−271.
(55) Sanchez-Fernandez, A.; Jackson, A. J.; Prévost, S. F.; Doutch, J. J.; Edler, K. J. Long-Range Electrostatic Colloidal Interactions and Specific Ion Effects in Deep Eutectic Solvents. *J. Am. Chem. Soc.* **2021**, *143*, 14158−14168.
(56) Kjellander, R. Nonlocal electrostatics in ionic liquids: The key to an understanding of the screening decay length and screened interactions. *J. Chem. Phys.* **2016**, *145*, 124503.
(57) Kjellander, R. Focus Article: Oscillatory and long-range monotonic exponential decays of electrostatic interactions in ionic liquids and other electrolytes: The significance of dielectric permittivity and renormalized charges. *J. Chem. Phys.* **2018**, *148*, 193701.
(58) Hu, Y.-S.; Lu, Y. The Mystery of Electrolyte Concentration: From Superhigh to Ultralow. *ACS Energy Lett.* **2020**, *5*, 3633−3636.
(59) Kremer, L. S.; Danner, T.; Hein, S.; Hoffmann, A.; Prifling, B.; Schmidt, V.; Latz, A.; Wohlfahrt-Mehrens, M. Influence of the Electrolyte Salt Concentration on the Rate Capability of Ultra-Thick NCM 622 Electrodes. *Batteries Supercaps* **2020**, *3*, 1172−1182.
(60) Larsen, H. Chapter 3 Ecology of Hypersaline Environments. In *Developments in Sedimentology*; Nissenbaum, A., Ed. Elsevier B. V., 1980; pp. 23−29.
(61) Woolard, C. R.; Irvine, R. L. Treatment of hypersaline wastewater in the sequencing batch reactor. *Water Res.* **1995**, *29*, 1159−1168.
(62) Everts, J. C.; Senyuk, B.; Mundoor, H.; Ravnik, M.; Smalyukh, I. I. Anisotropic electrostatic screening of charged colloids in nematic solvents. *Sci. Adv.* **2021**, *7*, eabd0662.

https://doi.org/10.1021/acs.langmuir.2c00519
Langmuir 2022, 38, 6164−6173